ELSEVIER

Mechanisms and Processes Leading to Changes in Time in the Properties of CFRC

Amnon Katz and Arnon Bentur
National Building Research Institute, Department of Civil Engineering, Technion—Israel Institute of Technology, Haifa, Israel

A study of carbon fiber reinforced cement (CFRC) composite produced from a dense matrix (low water:cement ratio, increasing content of silica-fume) indicated that it might undergo an aging effect, exhibited by an increase in strength and toughness at early age, followed by a reduction thereafter. This aging effect was not accompanied by corrosion of the fiber or the matrix, and an analytical model was developed to account for it based on processes of physical interaction between the fiber and the matrix.

The processes identified and quantified were: (1) nonuniform fiber length induced by fiber breakage during mixing; (2) increase in fiber-matrix bond with time; and (3) flexural stresses induced in inclined fibers bridging matrix cracks, leading to fiber failure as the matrix becomes denser with age and with increase in silica-fume content. ADVANCED CEMENT BASED MATERIALS 1996, 3, 1–13

KEY WORDS: Aging, Carbon fiber, Cement, Composite, Fiber bending breakage, Fiber mixing breakage

In a previous publication [1], it was shown that carbon fiber reinforced cement (CFRC) composites can undergo considerable changes in their properties when exposed to aging in water. The changes were characterized by increases in flexural strength and toughness to a maximum after 2 to 4 weeks, followed by reductions in both properties thereafter, to values which are 30 to 60% smaller than the early age maximum. Typical trends of this kind are presented in Figure 1. It was shown that the relative changes in flexural strength and toughness were similar and that the extent of loss in both properties after the early age maximum was higher in matrices of higher silica-fume content (for equal water:binder ratio) and for aging in water at higher temperature (60°C relative to 20°C). In addition, it was found that a maximum in flexural strength and toughness was achieved when densifying the matrix by using a moderate amount of silica-fume (~14% of the binder); a reduction in properties was observed for higher contents of silica-fume [2].

Scanning electron microscopy (SEM) observations did not reveal any signs of chemical deterioration of the fibers, in agreement with other studies [3,4]. The matrix itself was gaining strength even in the time periods when the composite was losing strength and toughness.

These results suggest that CFRC composites can undergo aging effects that are characterized by three main features:

1. Aging effect is similar from the point of view of loss in flexural strength and toughness.
2. More severe aging is obtained under conditions leading to greater densification of the matrix (high silica-fume content and higher aging temperature).
3. The aging is not accompanied by chemical deterioration of the fiber or the matrix.

These trends are quite different from aging observed in other cementitious composites. They cannot be correlated with any deterioration of the fiber and the matrix, but they seem to be associated with physical densening of the matrix. The object of the present paper was to resolve the mechanisms leading to these changes in properties that are associated with physical effects only and to establish an analytical model to quantify them.

Review of Models Accounting for Loss in Properties of Cementitious Composites Due to Physical Effects

The first mechanism accounting for the loss in properties of CFRC is fiber breakage in the mixing process. In most fiber reinforced concretes (FRCs), short fibers are

Address correspondence to: Arnon Bentur, National Building Research Institute, Technion City, Haifa 32000, Israel.
Received August 1, 1994; Accepted October 24, 1994

ISSN 1065-7355/96/$15.00
SSDI 1065-7355(95)00015-J

Advn Cem Bas Mat
1996;3:1–13

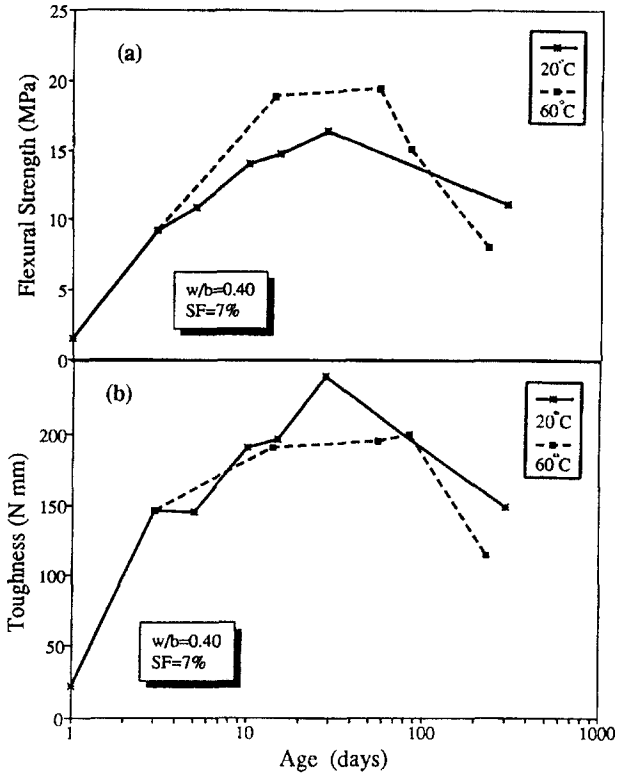

FIGURE 1. Effect of age on the mechanical properties of carbon fiber reinforced composite. The matrix water:binder ratio is 0.40 with 7% of silica-fume and 6% by volume of short carbon fiber, aged continuously in water at 20°C and 60°C. (a) Flexural strength; (b) fracture energy.

incorporated into the matrix during the mixing process. For brittle fibers, such as the carbon fibers, mixing induces intensive fiber breakage. It was found by Nishioka et al. [5] and Linton et al. [6] that fiber breakage occurs during mixing, and its intensity is affected by fiber strength and modulus, as well as the intensity of the mixing process.

It was shown by Laws [7] that changing the fiber length may change the composite strength and toughness, but these calculations were based on the assumption of a uniform fiber length. For carbon fibers, the length of the fiber after mixing is not uniform and varies over a wide range, which must be considered when calculating the composite properties.

The second mechanism is fiber bending while a stiff and brittle fiber bridges over a matrix crack. In the conventional approach to cementitious composites, fibers are considered to be bridging the crack at a constant angle along their axis [7,8], as shown in Figure 2a. Under such conditions, it can be shown that increase in fiber matrix bond will result in a continuous increase in tensile strength. Toughness will also increase, but only up to a critical bond value, and thereafter it will decrease where failure mechanism is changed from fiber pullout to fiber failure [9].

Such calculations do not take into consideration local bending of a fiber bridging a matrix crack, which is generated due to geometrical constraints imposed when the crack opens (see Figure 2b). This local bending can result in different types of influences, depending on the nature of the fiber—whether it is brittle or ductile, due to premature failure in bending. Aveston et al. [10] pointed out that for a brittle fiber the local stress due to bending may increase relative to the axial stress in aligned fiber by a factor of as much as 7 and 15 for glass and carbon fiber, respectively. This implies that the efficiency of the fiber is reduced considerably compared to the value calculated assuming a constant angle of the fiber across the crack. Aveston et al. [10] con-

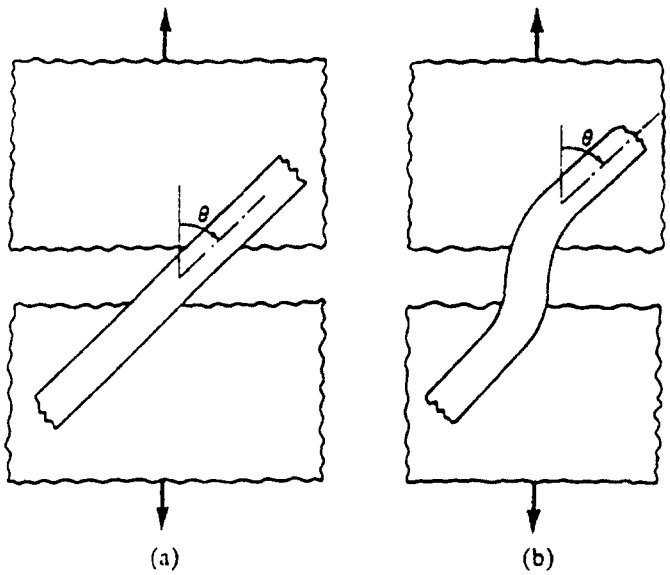

FIGURE 2. Schematic presentation of a fiber bridging a crack. (a) Straight fiber; (b) bending of the bridging fiber.

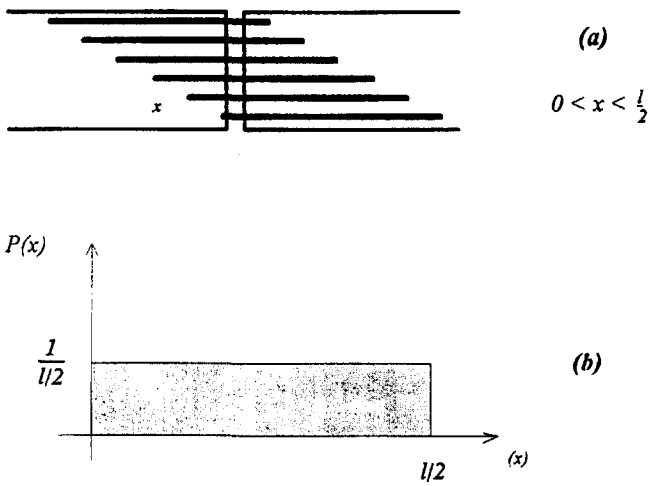

FIGURE 3. Fiber embedment length beyond the crack (a) and the probability function of the distribution of the embedment length (b), assuming uniform fiber length.

cluded that local crumbling (yielding) of the matrix can relax some of the bending stress induced in the fiber, and thus prevent at least part of the loss of the efficiency due to local bending. However, they did not propose a quantitative model to account for the fiber-matrix interaction.

The combined effect of matrix spalling and fiber bending stress was investigated lately by Leung and Li [11] who considered the fiber as a continuous beam supported by an elastic foundation (the matrix) of varied stiffness. They solved the problem by using finite elements methods together with very high computer power. According to their calculations, the bending stress in the fiber (expressed as strain) reaches a maximum at approximately 45°, and together with direct tensile stress the efficiency of the fiber may be reduced.

Stuck and Majumdar [12] and Bentur [13] suggested a similar explanation for the reduction in the properties of glass fiber reinforced cements during aging in addition to the chemical deterioration of the fibers. They proposed that as the matrix around the fiber becomes denser in time, the fiber loses its flexibility and the buildup of the bending stress is enhanced, leading to premature failure. The same problem was treated by Morton and Groves [14], Brandt [15], and Li et al. [16] for ductile fibers. Local yielding of the fiber at the bending points may increase the efficiency of the fibers, in contrast to such an effect in a brittle fiber. Li et al. [16] proposed the pulley mechanism that acts as an enhancement mechanism to the friction bond between the fiber and the matrix.

This brief review indicates that the fiber-matrix interaction can be quite complex and the nature of the fibers (brittle versus ductile) should be taken into account when analyzing the development of local bending. Such concepts were used in the present paper to develop an analytical model to account for the changes in properties of CFRC with time, as shown in Figure 1 and in the previous publications.

Analytical Model

Effect of Bond Strength and Fiber Length

FIBER LENGTH DISTRIBUTION. The strength and toughness of a cracked composite are determined by summing the tensile strength $\sigma(x)$ or pullout work $W(x)$ of a single fiber (x stands for the embedment length of the fiber into the matrix over the crack) for all the fibers bridging the crack. The embedded length is different for each of the bridging fibers. If the probability function of the embedment length, $p(x)$, is known, it can be expressed as follows:

$$\sigma = n\int\sigma(x)\, p(x)\, dx \tag{1}$$

$$W = n\int W(x)\, p(x)\, dx \tag{2}$$

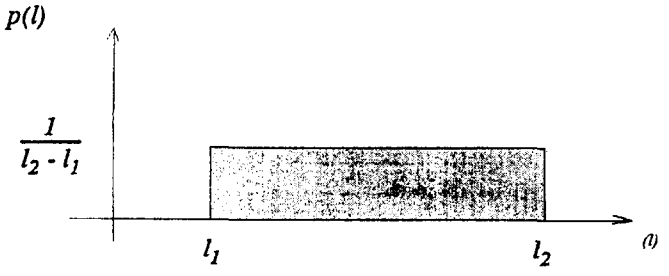

FIGURE 4. Probability density function of fiber length distribution using uniform distribution between length l_1 and l_2 of fibers of length l_2, which were broken during mixing.

Advn Cem Bas Mat
1996;3:1-13

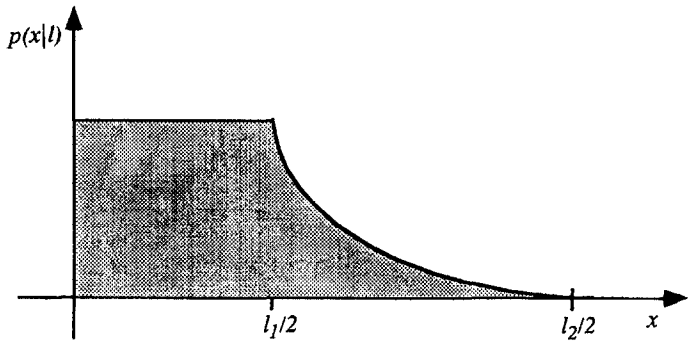

FIGURE 5. Probability function of the embedment length of a fiber bridging a crack, of fibers of nonuniform length distribution.

where x is the fiber embedded length and n is the number of fibers in a cross section, $n = V_f/(\pi d^2/4)$.

The integral in the equations represents the calculation of the average stress and pullout work of a single fiber, respectively. In the following, only the average stress and pullout work will be considered, as n is constant for a given fiber diameter and load.

Previous models [7,9,17,18] used the assumption of a uniform fiber length, thus the embedment length of the fiber beyond the crack varies uniformly between 0 and $l/2$ (l is fiber length) as shown schematically in Figure 3. In this case, $p(x)$ is a uniform distribution of the embedment length described by eq 3.

$$p(x) = \frac{1}{l/2} \qquad 0 < x < l/2 \tag{3}$$

Observations of fiber length distribution before and after mixing by Nishioka et al. [5] and Linton et al. [6] showed that fiber breakage occurs during mixing and fiber length varies widely depending on fiber properties and the mixing process. Thus, since the fiber length is not uniform, eq 3 is not applicable and the fiber length itself turns into a statistical parameter. To account for the length distribution, it was assumed that the length of the fibers broken during mixing is uniformly distributed between a minimum length l_1, which represents the shortest fiber obtained after breakage in mixing, and length l_2, which is the initial length representing a fiber which did not break during mixing (Figure 4 and eq 4). This assumption can reasonably represent the distribution reported by Nishioka et al. [5] and Linton et al. [6] and the data obtained by Katz [19]:

$$p(l) = \frac{1}{l_2 - l_1} \qquad l_1 < l < l_2 \tag{4}$$

where $p(l)$ is the probability function of the distribution of fiber length.

For an individual fiber of length l bridging a crack, the probability of the embedment length is of a uniform distribution at the range of $0 < x < l/2$. However, when mixing breakage is considered, the length l itself is a statistical variable that varies uniformly between l_1 and l_2 (eq 4).

The combined probability function for l and x is presented in eq 5:

$$p(x,l) = p(l)\,p(x) = \frac{1}{l_2 - l_1}\frac{2}{l} \tag{5}$$

Integration of the combined probability function over all the fiber lengths yields an expression for the probability function of the embedment length x:

$$p(x \mid l) = \begin{cases} \displaystyle\int_{l_1}^{l_2} \frac{1}{l_2 - l_1}\frac{2}{l}\,dl & 0 \leq x \leq l_1/2 \\ \displaystyle\int_{2x}^{l_2} \frac{1}{l_2 - l_1}\frac{2}{l}\,dl & l_1/2 \leq x \leq l_2/2 \end{cases} \tag{6}$$

The integration is done separately for two ranges of x. For embedment length shorter than $l_1/2$, all the fibers can provide contribution and, therefore, the integration limits are from l_1 to l_2. For longer embedment length, only fibers longer than twice the embedment length ($2x$)

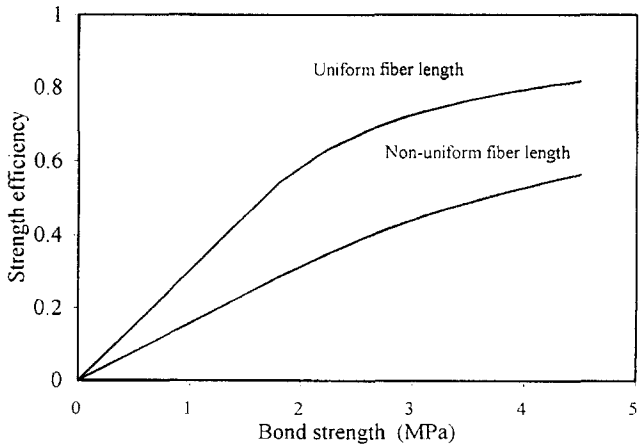

FIGURE 6. Effect of fiber-matrix bond strength on the strength efficiency of the fiber for uniform (l = 6 mm) and nonuniform (l = 0.25–6 mm) fiber length distribution.

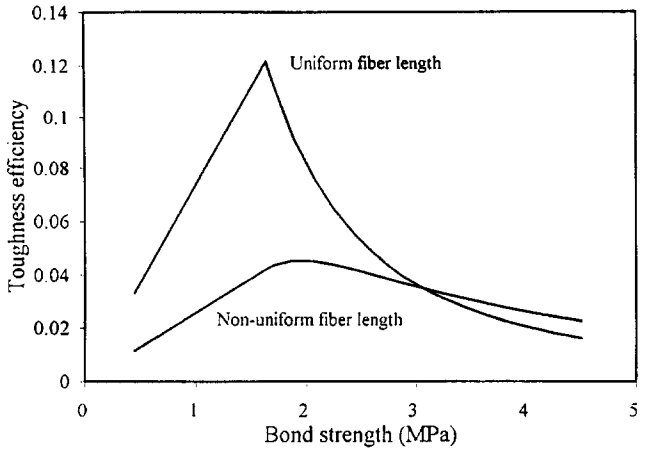

FIGURE 7. Effect of bond strength on the toughness efficiency of fibers of uniform and nonuniform length distribution.

can be considered for the integration, as shorter fibers can not provide any contribution. The integration limits for this case are from $2x$ to l_2.

The solution for the integral in eq 6 appears in eq 7 and is described in Figure 5.

$$p(x \mid l) = \begin{cases} \dfrac{2\,ln\dfrac{l_2}{l_1}}{l_2 - l_1} & 0 \leq x \leq l_1/2 \\ \dfrac{2\,ln\dfrac{l_2}{2x}}{l_2 - l_1} & l_1/2 \leq x \leq l_2/2 \end{cases} \tag{7}$$

Verifying this function was done by integrating eq 7 for all values of x (from 0 to $l_2/2$). The result was 1 as for all probability functions.

EFFECT OF FIBER LENGTH DISTRIBUTION ON THE STRENGTH AND TOUGHNESS. Introducing the probability function for the embedment length into eq 1 and 2 yields the effect of variation in fiber length on the mechanical properties of the composite. The maximum tensile stress developed in a fiber embedded in a matrix at a length x, assuming uniform distribution of bond stress along the fiber [20,21], is:

$$\sigma(x) = \frac{4\tau}{d} x \tag{8}$$

For calculation of the effect of the fiber length variation, eqs 7 and 8 are introduced into eq 1, leading to the following equation:

$$\sigma_{avg} = \begin{cases} \displaystyle\int_0^{l_1/2} \frac{4\tau}{d} x \frac{2\,ln\dfrac{l_2}{l_1}}{l_2 - l_1} dx & 0 \leq x \leq l_1/2 \\ \displaystyle\int_{l_1/2}^{l_2/2} \frac{4\tau}{d} x \frac{2\,ln\dfrac{l_2}{2x}}{l_2 - l_1} dx & l_1/2 \leq x \leq l_2/2 \end{cases} \tag{9}$$

Two different cases must be considered when solving eq. 9:

1. Bond strength is lower than the critical bond (the critical bond, τ_c, is calculated for the longest fiber l_2: $\tau_c = \sigma_f d \,/\, 2l_2$). In this case, all the fibers pull out, so the upper limit of the integral is $l_2/2$. The solution of eq 9 for this case is:

$$\sigma_{avg} = \frac{\tau}{d} \frac{l_2 + l_1}{2} \qquad \tau < \tau_c \tag{10}$$

2. Bond strength is higher than the critical bond. In this case, all fibers embedded in a length that is shorter than l_c will be pulled out and the stress in these fibers will be less than the fiber ultimate stress σ_f. For all fibers embedded in length that varies from $l_c/2$ to $l_2/2$, the stress is σ_f. l_c is calculated for each bond strength, τ, according to eq 11:

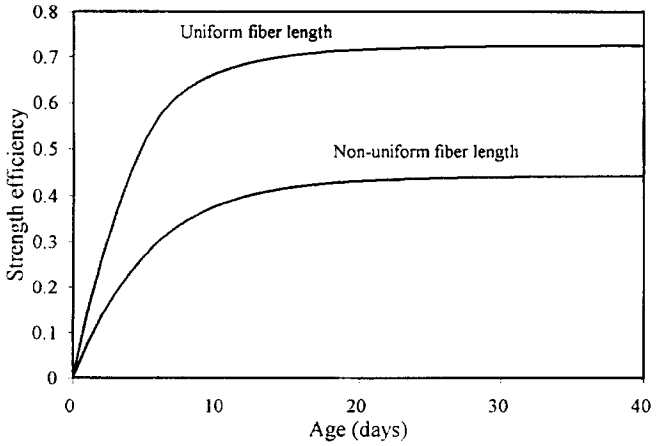

FIGURE 8. Fiber strength efficiency as a function of age, for carbon fiber reinforced concrete composite with uniform and nonuniform fiber length distribution.

Advn Cem Bas Mat
1996;3:1–13

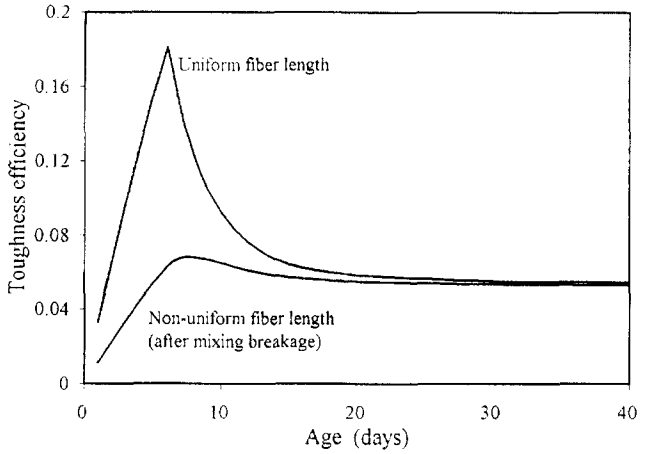

FIGURE 9. Toughness efficiency as a function of time, for carbon fiber reinforced concrete composites with uniform and nonuniform fiber length distribution.

$$l_c = \frac{\sigma_f d}{2\tau} \tag{11}$$

The solution of eq 9 for $\tau > \tau_c$ is:

$$\sigma_{avg} = \frac{\tau}{d(l_2 - l_1)} \left(l_c^2 \ln\frac{l_c}{l_2} + \frac{l_c^2 - l_1^2}{2} + 2l_c(l_2 - l_c) \right) \qquad \tau > \tau_c \tag{12}$$

The effect of the change in bond strength on the ratio of σ_{avg}/σ_f (which is the definition of the efficiency of the fiber in tension) is represented in Figure 6 for the case of uniform and nonuniform fiber length distribution. The parameters used for Figure 6 are based on fiber parameter characteristics for the CFRC composite studied here (E_f = 230 GPa, σ_f = 2,900 MPa, d = 6.8 μm, l_1 = 0.25 mm, and l_2 = 6 mm).

It can be seen from Figure 6 that the efficiency of short fibers is lower than 1, as there are always some fibers bridging the crack that are embedded in a length shorter than l_c. The efficiency of fibers of nonuniform distribution is obviously much lower.

The same considerations can be applied for determining the effect of the variation of fiber length on the toughness. The basic assumption for this case is that the toughness is affected mainly by the pullout work of the fiber from the matrix, while the other energies involved in the process are negligible [9,17]. The pullout work of a single fiber, embedded in the matrix at a length of x, is:

$$W(x) = \frac{1}{2}\pi\tau d x^2 \tag{13}$$

Introducing eq 13 together with eq 7 into eq 2 yields:

$$W_{avg} = \begin{cases} \int_0^{l_1/2} \frac{1}{2}\pi\tau d x^2 \frac{2\ln\frac{l_2}{l_1}}{l_2 - l_1} dx & 0 \le x \le l_1/2 \\ \int_{l_1/2}^{l_2/2} \frac{1}{2}\pi\tau d x^2 \frac{2\ln\frac{l_2}{2x}}{l_2 - l_1} dx & l_1/2 \le x \le l_2/2 \end{cases} \tag{14}$$

Here, too, two ranges of τ were considered:

1. $\tau < \tau_c$. When the bond strength is lower than the critical bond strength (calculated for the longest fiber l_2) all fibers are pulled out and contribute to the pullout work. The integration is done for the whole range of the fibers ($0 < x < l_2/2$). Equation 15 represents the solution of eq 14 for this case:

$$W_{avg} = \frac{1}{72}\pi\tau d\,(l_1^2 + l_1 l_2 + l_2^2) \qquad \tau < \tau_c \tag{15}$$

Introducing the case of uniform fiber length ($l_1 = l_2$) into eq 15 yields an equation similar to the one in Ramachandran et al. [22]. On the other hand, if the fibers break down to very small pieces, then $l_1 \to 0$ and the average pullout work will be one-third of the pullout work of a composite having uniform length l_2. This points out a severe reduction in the toughness as mixing breakage occurs.

2. $\tau > \tau_c$. When the bond strength is higher than the critical bond strength, all fibers embedded at

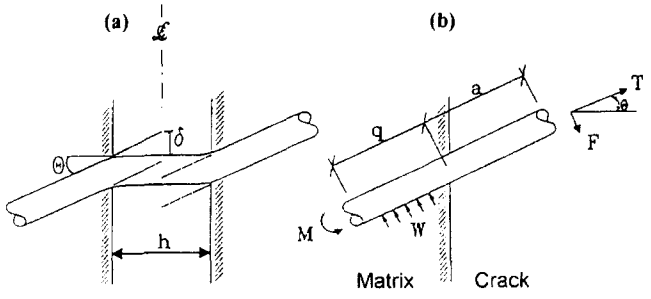

FIGURE 10. A model to describe the bending of an inclined fiber.

length shorter than l_c (calculated by eq 11) will be pulled out and will contribute to the toughness. All fibers embedded at length longer than l_c will break down and will not contribute to the toughness. The upper limit for the integral in eq 14 is therefore $l_c/2$ instead of $l_2/2$ and the solution is expressed in eq 16.

$$W_{avg} = \frac{\pi\tau d}{24(l_2 - l_1)}\left(l_c^3 \ln\frac{l_2}{l_c} + \frac{l_c^3 - l_1^3}{3}\right) \qquad \tau > \tau_c \tag{16}$$

The solutions for eqs 15 and 16 are presented in Figure 7, which demonstrates the effect of bond strength on the toughness efficiency for the case of uniform and nonuniform fiber length distribution. The toughness efficiency is the average pullout work of the bridging fibers embedded at various lengths (see eq 7) relative to the pullout work of a single fiber that is embedded in the matrix for half of its nominal length.

It seems that for both cases the trends are similar: an increase in the toughness as the bond increases up to a critical value at τ_c and a reduction thereafter. However, the sharp peak and transition in the case of uniform fiber length becomes more moderate as fiber length is nonuniform. The peak point at τ_c is much lower, and the composite can absorb less energy at this point. On the other hand, for the case of $\tau \gg \tau_c$, the existence of short fibers may contribute to the toughness of the composite. At this range of τ, these composites may show higher toughness than composites of uniform fiber length distribution.

AGE EFFECT. The bond strength is expected to increase in time, starting from zero at casting time, up to a final value, τ_∞, after prolonged hydration. To evaluate the effect of changes in bond strength in time on the composite properties, it was assumed that the bond strength develops at the same rate as the compressive strength of a cementitious matrix. An exponential function was fitted to compressive strength results of Goldman [23], leading to the following expression for τ:

$$\tau(t) = \tau_\infty\,(1 - e^{-0.17t}) \tag{17}$$

where t = time (days).

Figures 8 and 9 represent the effect of age on the strength and toughness of the composite, respectively. The calculations were performed for τ_∞ = 3.0 MPa, a value that was found by Larson et al. [24] in pullout tests, and other fiber parameters as indicated before. Both strength and toughness are expressed in relative values as explained before, representing the change in the efficiency of the fibers.

It can be seen from Figure 8 that the development of the composite strength is rapid at the first 2 to 3 weeks. When fiber mixing breakage occurs, the fibers are shorter than the nominal value, leading to less effective use of the fiber and lower composite strength.

For the toughness, as represented in Figure 9, the effect is different. For a uniform fiber length, toughness increases rapidly at the early age until the bond reaches its critical value, and thereafter it decreases. As fiber mixing breakage occurs, the toughness increases to a value that is approximately only one-third of the toughness of a uniform fiber length composite. However, the reduction after this peak is moderate, and the composite does not lose much of its toughness as occurs for the case of uniform fiber length.

Effect of Fiber Bending and Age

FIBER BENDING. The model was developed based on the assumptions of Morton and Groves [14] and Morton [25]. According to this model, the problem of inclined fiber bridging matrix crack is symmetric for both sides of the crack, as shown in Figure 10a. Therefore, it is possible to cut the fiber in the symmetry line and induce a load F (Figure 10b) in order to bend the fiber by a displacement δ back to the position providing continuity of the whole fiber across the crack.

As a result of the bridging stress in the fiber, a local reaction, w, in the matrix is developed over a length of q (which will be referred to later as length of support). Under these conditions, the fiber is subjected to a moment M. As can be seen from Figure 10b, the fiber is considered as a cantilevered beam having a free length of a. The value of a depends on several geometric parameters: crack width, h; fiber diameter, d; and the inclination angle θ (eq 18):

$$a = \frac{h}{2}\cos\theta + \frac{d}{2}\tan\theta \tag{18}$$

The bending moment, M_b, along the fiber is:

$$M_b = \begin{cases} Fx & 0 < x < a \\ Fx - \dfrac{w(x-a)^2}{2} & a < x < a + q \end{cases} \tag{19}$$

where x is the distance from the symmetry line, that is, the apparent free edge of the fiber.

This moment has a maximum at $x = a + q$, with a value of:

$$M_{max} = F(a+q) - \frac{1}{2}wq^2 \tag{20}$$

By double integration of the moment in eq 19, and

Advn Cem Bas Mat
1996;3:1–13

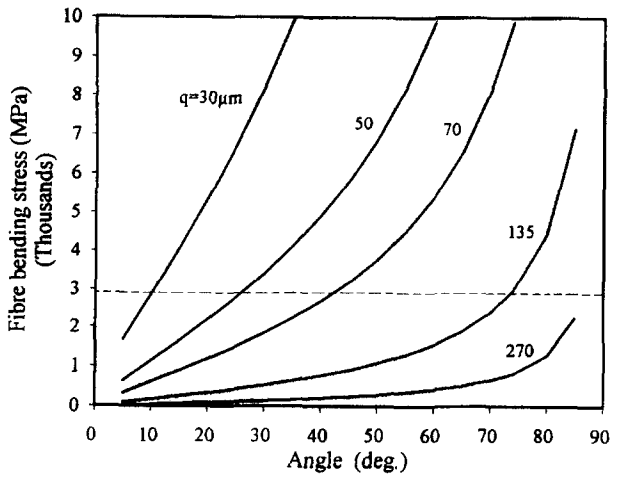

FIGURE 11. Effect of angle on the bending stress for different lengths of support.

adding boundary condition of $(dy)/(dx) = 0$ at $x = a + q$, it is possible to express the deflection, δ, at the symmetry line (i.e., $x = 0$):

$$\delta = \frac{1}{E_f I_f}\left(\frac{F}{3}(a+q)^3 - \frac{1}{8}wq^4 - \frac{1}{6}wq^3a\right) \tag{21}$$

where E_f, I_f are modulus of elasticity and moment of inertia of the fiber, respectively.

The above treatment of Morton and Groves was further developed to calculate the bending stress in the fiber.

From balance of loads:

$$w = \frac{F}{q} \tag{22}$$

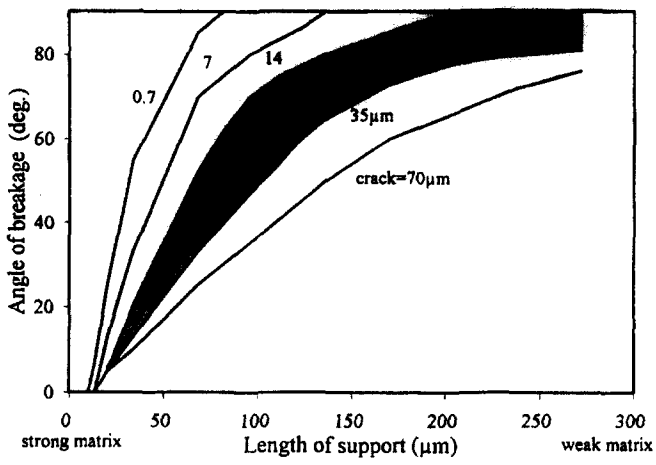

FIGURE 12. Effect of length of support on the bending breakage angle (θ_b) of the fiber, for different crack widths.

Introducing w from eq 22 into eq 21 yields an expression for the load F:

$$F = \frac{E_f I_f \delta}{\frac{1}{3}(a+q)^3 - \frac{1}{8}q^3 - \frac{1}{6}q^2a} \tag{23}$$

where $\delta = 0.5h \tan \theta$.

Introducing w from eq 22 into eq 20 yields an expression for the maximum moment M_{max}:

$$M_{max} = F\left(a + \frac{1}{2}q\right) \tag{24}$$

The bending stress, σ_b, in the fiber is therefore:

$$\sigma_b = \frac{M}{I_f}\frac{d}{2} = \frac{E_f \frac{1}{2} d\delta\left(a + \frac{1}{2}q\right)}{\frac{1}{3}(a+q)^3 - \frac{1}{8}q^3 - \frac{1}{6}q^2a} \tag{25}$$

This equation expresses the bending stress in the fiber as function of the fiber parameters (modulus of elasticity E_f, and diameter d), matrix parameter (length of support q), and geometry (crack width h, and angle θ).

Morton and Groves [14] suggested that w, the matrix reaction, is proportional to the microhardness H (eq 26), as the latter is an indication of the properties of the matrix in the vicinity of the fiber and is supposed to represent a value related to the maximum stress that might develop in the matrix. Yet, in view of differences between the ideal description of the model and the actual behavior, accounting for effects such as three-dimensional stress field and nonuniform stress distribution of w, this assumption may not be accurate enough to be directly introduced into the equations.

$$w = H \cdot d \tag{26}$$

Substituting eq 26 into eq 22 results in:

$$F = H\, d\, q \tag{27}$$

which can represent schematically the relationship between the matrix properties expressed in terms of the microhardness H and the parameter q used in the model. It can be seen that for a given bending load F, needed to deflect the fiber, the use of strong matrix (high values of H) results in a short length of support, and vice versa: Weak matrix is represented by large values of q.

Figure 11 represents the solution for bending stresses developed in a fiber having parameters of the carbon fibers tested in this work, as a function of the inclination

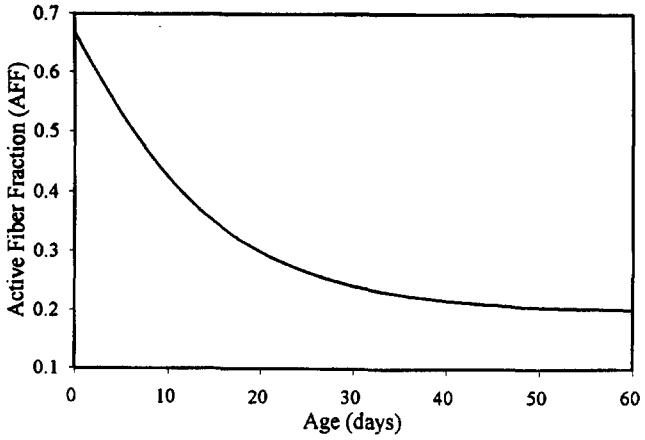

FIGURE 13. Effect of time on reduction of the active fiber fraction, AFF, due to bending effect, calculated using eq 31 with q_0 = 100 μm and q_∞ = 35 μm.

angle, θ, for the case of crack width of 20 μm and different lengths of support q.

It can be seen that for a fixed length of support, the bending stress increases with the angle. For the same angle, the bending stress in the fiber for a matrix having a long length of support (weak matrix) is much lower than the bending stress in a fiber in a matrix having a short length of support (i.e., dense and strong matrix). The dotted line in Figure 11 represents the ultimate strength of the fiber studied. Actually, as a brittle fiber is subjected to a stress exceeding this limit, it will fail in bending and will not contribute to the composite properties.

Therefore, it is possible to define the breakage angle, θ_b, as the angle at which the fiber fails in bending. This angle is a function of q and the crack widths. Results of calculations of θ_b are presented in Figure 12. The calculation was done by a numerical solution of eq 25, for fiber strength of 2,900 MPa, which is typical to the carbon fiber that was used in the experimental study. The numerical solution is required here as the angle, θ, is not a direct parameter in the equation but appears in the equations of a and δ (eqs 18 and 23, respectively). The different lines in Figure 12 represent solution for different crack widths. The shaded area represents a range of crack width of 15–35 μm, which is the typical crack width observed microscopically for the materials investigated in this study. It seems that this range is relatively narrow and can be represented by a single characteristic line having the following equation:

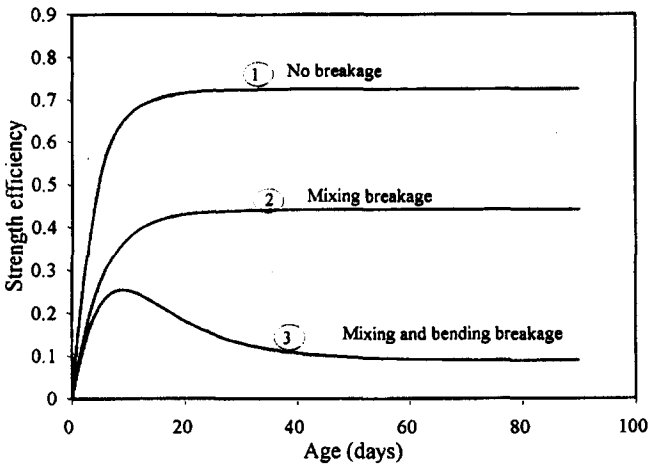

FIGURE 14. Strength efficiency as function of time: (1) influence of bond only, assuming uniform fiber length (i.e., no breakage during mixing); (2) influence of bond only, assuming nonuniform fiber length (i.e., fiber breakage during mixing); and (3) combined influence of bond (assuming nonuniform fiber length) and bending.

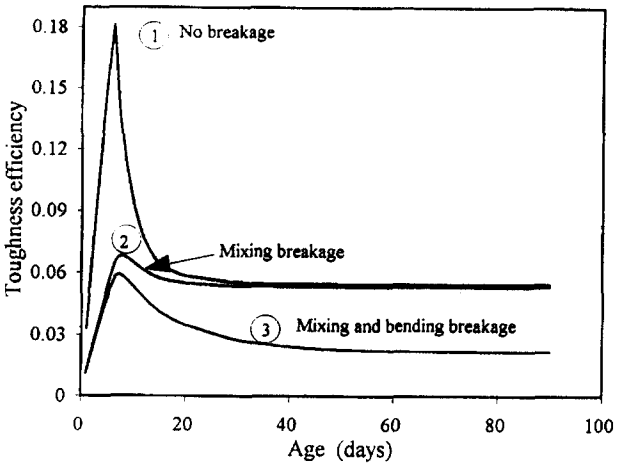

FIGURE 15. Toughness efficiency as function of time: (1) influence of bond only, assuming uniform fiber length (i.e., no breakage during mixing); (2) influence of bond only, assuming nonuniform fiber length (i.e., fiber breakage during mixing); and (3) combined influence of bond (assuming nonuniform fiber length) and bending.

$$\theta_b = \frac{\pi}{2}[1 - \exp(aq^b)] \tag{28}$$

where $a = -38.09$, $b = 1.536$, and q is expressed in millimeters.

Testing the sensitivity of the choice of this curve relative to the curves of crack width of 15 μm or 35 μm shows that the deviation of the chosen curve from the two extremes crack widths is 15% for most of the range of values of the length of support.

It can be seen from Figure 12 that a reduction in the length of support (i.e., increase in the hardness of the matrix), as may happen during aging of a cementitious matrix, leads to a reduction in the breakage angle. It should be noted that as all the fibers above this angle break in bending, only the fibers below this angle survive and are able to support load across the crack. For a uniform fiber distribution angle between 0 and $\pi/2$, as proposed by Perimi and Rao [26], the probability function of a fiber to have an inclination angle between 0 and θ_b is:

$$p(\theta) = \int_0^{\theta_b} \frac{d\theta}{\pi/2} = \frac{\theta_b}{\pi/2} \tag{29}$$

Substituting θ_b from eq 28 into eq 29 yields a relationship between the fraction of fiber inclined at an angle below θ_b (the active fiber fraction, AFF) and the length of support q for the carbon fibers studied in this work:

$$\text{AFF} = 1 - \exp(aq^b) \tag{30}$$

AGE EFFECT. As the matrix becomes denser and stronger in time, the length of support, q, is reduced, leading to a reduction in the fraction of fibers that are able to carry the bridging loads (i.e., reduction in AFF in eq 30). This in turn should lead to weakening of the composite. The reduction in the length of support was simulated by eq 31, which assumes that this process is developed at the same rate as the compressive strength of cementitious materials, similar to the estimation of the development of the bond strength presented earlier:

$$q(t) = q_\infty + (q_0 - q_\infty)e^{-0.0822t} \tag{31}$$

where q_0, q_∞ is length of support at $t = 0$ and $t = \infty$, respectively.

The effect of the reduction with the active fiber fraction in time, as the length of support reduces, is presented in Figure 13. For this figure, the values of q in eq 30 were calculated from eq 31 assuming $q_0 = 100$ μm (15 fiber diameters) and $q_\infty = 35$ μm (5 diameters). In practice, these values together with the rate of changes in q need to be determined for each particular case of matrix composition and curing conditions.

It can be seen from Figure 13 that as the hydration proceeds and the matrix becomes stronger and stiffer, the AFF is reduced, leading to loss in the efficiency of the fibers in the matrix with time.

Combined Effect of Bond and Bending on the Long-Term Behavior of the Composite

Two processes, opposing in nature that may lead to changes in the properties of the composite with time, were identified: the influence of bond (Figures 8 and 9) and fiber bending (Figure 13). Thus, the combination of the two, as they occur simultaneously, may lead to a

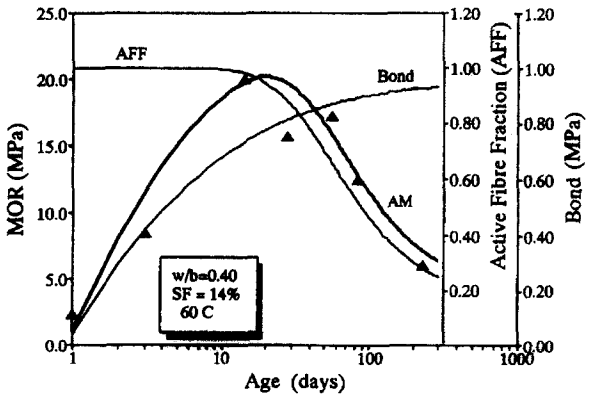

FIGURE 16. Combined influence of changes in efficiency due to the effect of bond (bond curve) and bending (AFF curve) to account for the experimental time dependent behavior of carbon fiber reinforced concrete composite (AM curve).

variety of effects on the strength and toughness, as seen in Figures 14 and 15, respectively.

It can be seen from Figure 14 that when using brittle fibers, the composite strength can be reduced: (1) Fiber mixing breakage, which leads to nonuniform fiber length shorter than the initial length, reduces the strength at all times (line 2 relative to line 1). (2) The influence of fiber bending breakage leads to additional reduction in strength with different effects at different ages. An initial increase in strength with time might be observed (line 3 in Figure 14); but later, as the effect of bending breakage increases, the active fiber fraction reduces, leading to a reduction in the composite strength at the late ages.

For the toughness, as presented in Figure 15, two regions of time must be considered. At early age, when the bond strength is below τ_c, the effect of time leads to an increase in the toughness due to the increase in bond. This increase is smaller when mixing breakage or bending breakage occurs. However, at later age, when $\tau > \tau_c$, all processes work together to reduce the toughness (line 3 relative to line 1), leading to a severe loss in toughness.

Aging Mechanisms in CFRC

The changes in properties during continuous water immersion at 20°C and 60°C of CFRC [1] as shown in Figure 1 might be explained on the basis of the two opposing processes described previously, both of which are associated with the densening of the matrix. The analytical models developed for these two processes were used to account quantitatively for the curves, as seen in Figure 16 for one typical case.

The procedure was based on numerical solution to find the time dependent function for AFF in eq 31 [i.e., AFF(t)] and for τ in eq 17 [i.e., $\tau(t)$] to provide the best fit to the actual experimental results. On the basis of this procedure, the time dependent curves for AFF and τ for each composition (i.e., silica-fume content) were found and are shown in Figures 17a and 17b, respectively.

It can be seen that the bond increases continuously with time and with the increase in the silica-fume content. Most of the increase in bond strength was gained when the silica-fume content increased from 0 to 7–14%. Higher silica-fume contents did not improve the bond significantly. This trend was similar at all ages. Bond

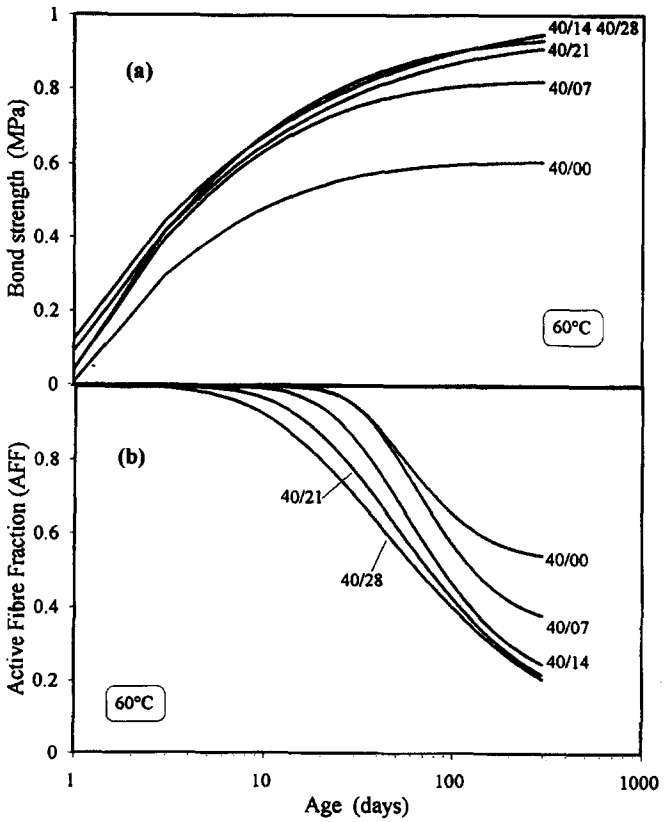

FIGURE 17. Effect of age and silica-fume content on the efficiency of fibers in carbon fiber reinforced concrete composite due to (a) bond and (b) bending (AFF factor) mechanisms; 0.40 water:binder ratio composite aged at 60°C.

values seem to be somewhat low (1.0–1.5 MPa) relative to the results of Larson et al. [24]. However, they are in good agreement with the results of Katz and Li [27] obtained by a special pullout technique designated for carbon fibers. The AFF seems to be reducing with age and with the increase in silica-fume content.

To resolve the influence of silica-fume, the AFF and τ (bond) values at early age (28 days) and later ages (230 days) were plotted as a function of silica-fume content (Figure 18). It can be seen that the influence of silica-fume on τ is quite similar at early and late ages: The bond increases rapidly for low silica-fume contents (up to 14%) and does not change much for higher silica-fume contents. The AFF factor seems to be much lower at later ages, and decreases at a higher rate with increase in silica-fume, compared to the trends in earlier age. These results clearly show that the combined increase in age and silica-fume had a greater relative influence on reduction in AFF than on increase in τ, thus accounting for the loss in properties during aging, which is more pronounced in higher silica-fume content composites.

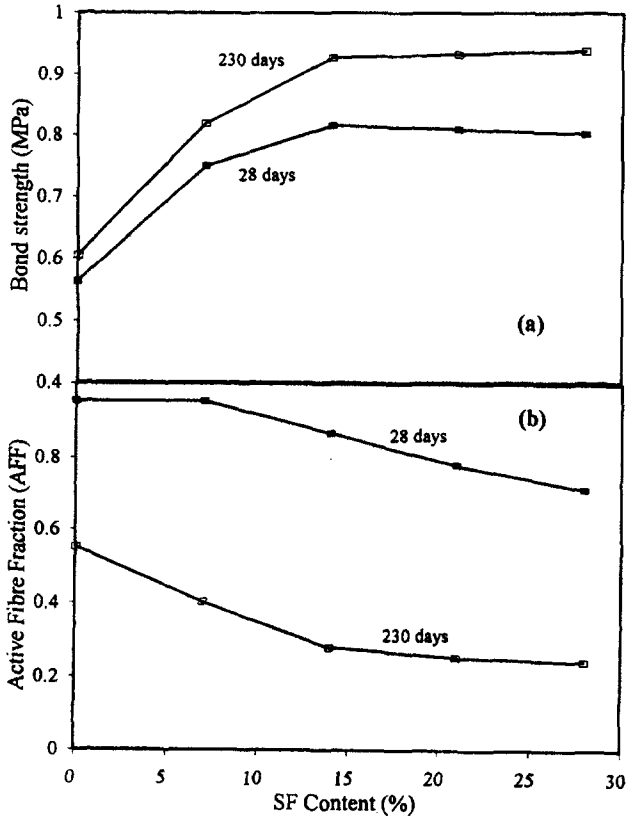

FIGURE 18. Effect of silica-fume content and age on characteristic values (bond and AFF) of the bond and aging mechanisms calculated from the experimental results on the basis of the analytical model.

Conclusions

CFRC products with dense matrix may undergo an aging effect that shows up by an increase in mechanical properties (strength and toughness) at early age and a reduction thereafter. These changes in properties were accounted for by an analytical model that considers the following effects. Variation in fiber length due to fiber breakage in mixing may lead to a severe reduction in the composite strength and toughness at all ages. The long-term properties of CFRC are controlled by two mechanisms: (1) an increase in the fiber-matrix bond due to matrix densening; and (2) a reduction in the active fiber fraction as the matrix becomes denser and stronger, due to fiber bending rupture. Low silica-fume content (up to 14% of the binder) improves the fiber-matrix bond considerably. Further increase in silica-fume content has only a moderate influence on increase in bond. At early age of 2 to 4 weeks, low silica-fume contents do not affect much the active fiber fraction (AFF), and only high content of silica-fume (above 14%) seems to reduce the AFF. However, at later ages, the increase in silica-fume content has a considerable influence on the reduction in AFF, in particular an increase from 0 to 14% of silica-fume.

References

1. Katz, A.; Bentur, A. *Int. J. Cem. Conc.*, in press.
2. Katz, A.; Bentur, A. *Cem. Concr. Res.* **1994,** *24,* 214–220.
3. Akihama, S.; Suenaga, T.; Bannot, T. *Mechanical Properties of Carbon Fiber Reinforced Cement Composites and the Application to Large Domes;* KICT Report No. 53, 1984; p 97.
4. Balaguru, P.N.; Shah, S.P. *Fiber Reinforced Cement Composites;* McGraw Hill: New York, 1992; p 530.
5. Nishioka, K.; Yamakawa, S.; Shirakawa, K. In *Developments in Fiber Reinforced Cement and Concrete, RILEM Symposium FRC 1986;* 1986; pp 79–88.
6. Linton, J.R.; Berneburg, P.L.; Gartner, E.M.; Bentur, A. In *Fiber Reinforced Cementitious Materials;* Mindess, S.; Skalny, J., Eds.; 1990; pp 255–264
7. Laws, V. *J. Phys. D. Appl. Phys.* **1971,** *4,* 1737–1746.
8. Allen, H.G. *J. Phys. D. Appl. Phys.* **1972,** *5,* 331–343.
9. Bentur, A.; Mindess, S. *Fiber Reinforced Cementitious Composites;* Elsevier Science Publishers: Amsterdam, 1990; p 449.
10. Aveston, J.; Mercer, R.A.; Sillwood, J.M. In *Composites, Standards Testing and Design, Proc. National Physical Laboratory Conference,* UK, 1974; pp 93–103.
11. Leung, C.K.Y.; Li, V.C. *J. Mech. Phys. Solids* **1992,** *40,* 1333–1362.
12. Stuck, M.S.; Majumdar, A.J. *J. Mater. Sci.* **1976,** *11,* 1019–1030.
13. Bentur, A. *Adv. Cem. Res.* **1988,** *1,* 147–154.
14. Morton, J.; Groves, G.W. *J. Mater. Sci.* **1976,** *9,* 1436–1445.
15. Brandt, A.M. In *Fiber Reinforced Concrete,* ACI SP-81; Hoff, G.C., Ed.; American Concrete Institute; Detroit, MI, 1984; pp 267–286.
16. Li, V.C.; Wang, Y.; Backer, S. *Composites* **1990,** *21,* 132–140.

17. Kelly, A. *Strong Solids,* 2nd ed. Clarendon Press: Oxford, 1973; p 285.
18. Li, V.C.; Wang, Y.; Backer, S. *J. Mech. Phys. Solids,* **1991,** *39,* 607–625.
19. Katz, A. *Composites of Fiber Reinforced High-Strength Cementitious Matrix,* D.Sc. Thesis; Technion: Haifa, Israel, 1992.
20. Wang, Y.; Backer, S.; Li, V.C. *J. Mater. Sci.* **1987,** *22,* 4281–4291.
21. Bartos, P. *Int. J. Cem. Comp.* **1981,** *3,* 159–177.
22. Ramachandran, V.S.; Feldman, R.F.; Beaudoin, J.J. *Concrete Science;* Hyden and Sons: London, 1981; 169–223.
23. Goldman, A. *The Behavior of a Cementitious System Containing Silica Fume,* D.Sc. Thesis; Technion IIT: Haifa, Israel, 1991.
24. Larson, B.K.; Drzel, L.T.; Sorousian, P. *Composites* **1990,** *21,* 205–215.
25. Morton, J. *Mater. Struct.* **1979,** *12,* 393–396.
26. Perimi, S.R.; Rao, J.K.S. *On the Fracture Toughness of Fiber Reinforced Concrete,* ACI SP-44-4; American Concrete Institute: Detroit, MI, 1973; 79–92.
27. Katz, A.; Li, V.C., Kazmer, A. *J. Mater. Civil Eng.* **1995,** *7,* 125–128.